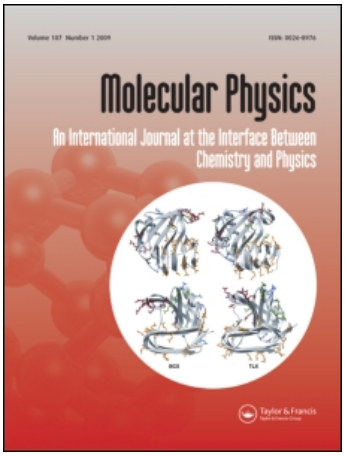

Molecular Physics
Publication details, including instructions for authors and subscription information:
http://www.informaworld.com/smpp/title~content=t713395160

A unified description of sum frequency generation, parametric down conversion and two-photon fluorescence

Oleksiy Roslyak [a]; Shaul Mukamel [a]
[a] Chemistry Department, University of California, Irvine, CA 92697-2025, USA

To cite this Article Roslyak, Oleksiy and Mukamel, Shaul(2009) 'A unified description of sum frequency generation, parametric down conversion and two-photon fluorescence', Molecular Physics, 107: 3, 265 — 280
To link to this Article: DOI: 10.1080/00268970902824250
URL: http://dx.doi.org/10.1080/00268970902824250

Molecular Physics
Vol. 107, No. 3, 10 February 2009, 265–280

Taylor & Francis
Taylor & Francis Group

RESEARCH ARTICLE

A unified description of sum frequency generation, parametric down conversion and two-photon fluorescence

Oleksiy Roslyak* and Shaul Mukamel

Chemistry Department, University of California, Irvine, CA 92697-2025, USA

(*Received 6 November 2008; final version received 13 February 2009*)

A superoperator non-equilibrium Green's function formalism is presented for computing nonlinear optical processes involving any combination of classical and quantum optical modes. Closed correlation-function expressions based on superoperator time-ordering are derived for the combined effects of causal response and non-causal spontaneous fluctuations. Coherent three wave mixing (sum frequency generation and parametric down conversion) involving one and two quantum optical modes, respectively, are compared with their incoherent counterparts: two-photon-induced fluorescence and two-photon-emitted fluorescence.

Keywords: *ab initio*; electronic structure; quantum chemistry; computational chemistry

1. Introduction

Quantum optics focuses primarily on the quantum properties of light [1–3]. When the optical fields are tuned off-resonance with respect to the matter transitions, the matter serves as mediator of interactions between the field modes. The optical processes may then be described by an effective Hamiltonian for the field [1,2], and the matter only enters through some parameters such as nth-order nonlinear susceptibilities $\chi^{(n)}$. The parametric description quantum of optics misses all resonant spectroscopic information.

Nonlinear spectroscopy, on the other hand, is mainly concerned with intrinsic properties of the material and uses classical light to interrogate them [4,5]. The semiclassical approach [2], which treats the material quantum mechanically and all fields classically, is broadly used in spectroscopic applications. When a quantum system interacts with a classical field its properties may be described by a set of *causal response functions* (CRF) which can be derived order by order in the coupling. These CRF are given by specific combinations of dipole correlation functions with various time orderings [4]. Causality, which implies that all interactions occur prior to the observation time, is guaranteed by their retarded nature. Strictly speaking, for spontaneous processes where the signal field is initially in the vacuum state, that mode must be treated quantum mechanically. This is avoided in the semiclassical approach to coherent nonlinear optics by computing the signal by solving Maxwell's equations; quantum fields are never introduced at this level of theory.

Quantum spectroscopy brings both worlds together by treating the light and matter as coupled quantum systems. When two quantum systems are placed in contact, they interact thorough spontaneous, non-causal, fluctuations. It is not possible to classify the dynamical events in terms of a cause and an effect. By working in Liouville space and introducing superoperator notation it is possible to describe processes involving any combination of classical and quantum optical modes in terms of a single set of superoperator non-equilibrium Green's functions (SNGF) [6–9]. The SNGF formalism is essential when some modes other than the signal mode are quantum. Once the quantum nature of the optical field is taken into account, the signals may not be represented solely by the CRFs since non-causal correlated spontaneous fluctuations of *both* matter and field must be taken into account. Optical signals can then be described by superoperator non-equilibrium Green's functions (SNGF), which are given by other combinations of dipole correlation functions.

In this paper we apply the SNGF formalism to establish the connections between various types of experiments involving quantum modes of the radiation field. All quantum modes considered here are initially in their vacuum states and are populated by

*Corresponding author. Email: oroslyak@uci.edu

ISSN 0026–8976 print/ISSN 1362–3028 online

DOI: 10.1080/00268970902824250
http://www.informaworld.com

spontaneous emission. Spectroscopy with other types of non-classical quantum fields including entangled photons will be reported elsewhere.

We first consider several coherent signals [8] which scale as $N(N-1)$, where N is the number of optically active molecules. These include homodyne-detected sum frequency generation (SFG) [10] and difference frequency generation (DFG) [4,11], which involve two classical and one quantum mode. We further calculate parametric down conversion (PDC) [12–15], which involves one classical and two quantum modes. PDC is one of the primary sources of entangled photon pairs [1,16,17].

We further consider incoherent signals which scale as N. These comprise heterodyne-detected SFG and DFG, which involve three classical modes, and two types of two-photon fluorescence [18]: two-photon-induced fluorescence with one classical and two quantum modes (TPIF) [19–21] and two-photon-emitted fluorescence with two classical and one quantum make (TPEF).

The semiclassical approach cannot describe the most general nonlinear optical processes which involve spontaneously generated photons. In contrast, the SNGF language of quantum spectroscopy can describe both quantum and classical optical fields. Seemingly different processes can then be treated by a unified formalism.

The SNGF allow us to classify the various possible measurements systematically and compare their information content. This formalism has been applied to describe Van Der Waals forces in molecules [6], charge transfer in quantum junctions [7] and inelastic resonances in STM currents [22]. A brief description of the SNGF is presented in the next section.

2. Quantum description of multiple wave mixing

We start with the quantized light–matter Hamiltonian

$$H(t) = H_0 + H_{\rm int}(t). \tag{1}$$

Here, H_0 is the material Hamiltonian. The field–matter coupling in the interaction picture with respect to the optical field is given by

$$H_{\rm int} = -\sum_\alpha E'_\alpha(t) V'_\alpha.$$

The quantized electric field operator of mode α is

$$E'_\alpha(t) = E_\alpha(t) + E^\dagger_\alpha(t). \tag{2}$$

Here,

$$E_\alpha(t) = \mathbf{e}_\alpha \sqrt{\frac{2\pi\hbar\omega_\alpha}{\Omega}} a_\alpha \exp\left(i\mathbf{k}_\alpha \mathbf{r} - i\omega_\alpha t\right)$$

is the positive frequency part and $\mathbf{e}_\alpha$, ω_α and $\mathbf{k}_\alpha$ are the polarization, frequency and wave vector of the given mode α, a_α is the photon annihilation operator and Ω is the quantization volume. The mode index spans a set $\alpha = \{|n\rangle_1, |n\rangle_2, \ldots\}$, where $|n\rangle_\alpha$ is an n photon state in mode α. Similar to Equation (2), the molecular transition dipole moment operator will be partitioned into positive and negative frequency components $V'_\alpha = V_\alpha + V^\dagger_\alpha$, where the subscript implies projection on the quantized electric field direction of mode α.

We assume that the detector registers the number of photons per unit time in mode α and the signal is given by the time-averaged photon flux:

$$S_\alpha = \lim_{T\to\infty} \frac{1}{2T} \int_{-T}^{T} \frac{\mathrm{d}}{\mathrm{d}t} \langle a^\dagger_\alpha a_\alpha \rangle \mathrm{d}t. \tag{3}$$

Using the Heisenberg equation of motion for the photon number in mode α,

$$\frac{\mathrm{d}}{\mathrm{d}t} a^\dagger_\alpha a_\alpha = \frac{i}{\hbar}[H_{\rm int}, a^\dagger_\alpha a_\alpha],$$

and the interaction Hamiltonian (1), the signal can be expressed as

$$S_\alpha = \frac{1}{\pi\hbar} \Im \int_{-\infty}^{\infty} \langle E'_\alpha(t) V'_\alpha(t) \rangle \mathrm{d}t, \tag{4}$$

where the explicit time dependence of the dipole operator is given in the interaction picture with respect to the molecular part of the Hamiltonian H_0 [8]. The expectation value $\langle \ldots \rangle$ is over the initial state of the entire matter/photon system at $t = -\infty$.

We next introduce the superoperator notation. With every ordinary operator A we associate two superoperators defined by their action on an ordinary operator X as $A_{\rm L} = AX$ (left), $A_{\rm R} = XA$ (right). We further define a different set of superoperators by a unitary transformation,

$$A_- = \frac{1}{\sqrt{2}}(A_{\rm L} - A_{\rm R}), \quad A_+ = \frac{1}{\sqrt{2}}(A_{\rm L} + A_{\rm R}).$$

More details on the superoperator algebra in the L,R and +, − representations are given in Appendix A [22].

The SNGF of nth order are defined as traces of time-ordered products of such superoperators:

$$\langle \mathcal{T} A_+(t) \underbrace{A_+(t_n) \ldots A_+(t_{n-m+1})}_{m} \underbrace{A_-(t_{m-n}) \ldots A_-(t_1)}_{n-m} \rangle,$$

where $m=0,\ldots,n$. The time-ordering superoperator is a key bookkeeping device in this formalism and is defined as

$$\mathcal{T}A_{\nu_1}(t_2)B_{\nu_2}(t_1)=\theta(t_2-t_1)A_{\nu_1}(t_2)B_{\nu_2}(t_1)+\theta(t_1-t_2)B_{\nu_2}(t_1)A_{\nu_1}(t_2).$$

The indices ν_j can be either + or −, and $\theta(t)$ is the Heaviside step function. The SNGFs may contain an arbitrary number of + and − superoperators. The chronologically last superoperator must be a + one, otherwise the SNGF vanishes (see Equation (A3)).

The signal (4) can be expanded perturbatively $S_\alpha=\sum_{m=1}^{\infty}S_\alpha^{(m)}$ in the interaction superoperator H_-^{int} (see Appendix A).

The material SNGFs are defined as

$$\mathbb{V}^{(m)}_{\nu_{m+1}\nu_m\ldots\nu_1}(t_{m+1},t_m,\ldots,t_1)=\left\langle\mathcal{T}V'_{\nu_{m+1}}(t_{m+1})V'_{\nu_m}(t_m)\ldots V'_{\nu_1}(t_1)\right\rangle. \tag{5}$$

The causal response functions (CRFs) are one type of SNGF and have the form $\langle A_+(t)A_-(t_n)\ldots A_-(t_1)\rangle$ (one + and several − superoperators). SNGFs of the form

$$\mathbb{V}^{(m)}_{+\underbrace{-\cdots-}_{m}}$$

give a causal ordinary molecular response function of mth order. The material SNGFs of the form

$$\mathbb{V}^{(m)}_{+\underbrace{+\cdots+}_{m}}$$

represent the mth moment of the fluctuating molecular superoperator. Material SNGF of the form

$$\mathbb{V}^{(m)}_{+\underbrace{+\cdots+}_{n}\underbrace{-\cdots-}_{m-n}}$$

indicates changes in the nth moment of molecular fluctuations induced by $m-n$ light/matter interactions [6].

The optical field SNGFs are defined similarly:

$$\mathbb{E}^{(m)}_{\nu_{m+1}\nu_m\ldots\nu_1}(t_{m+1},t_m,\ldots,t_1)=\left\langle\mathcal{T}E'_{\nu_{m+1}}(t_{m+1})E'_{\bar{\nu}_m}(t_m)\ldots E'_{\bar{\nu}_1}(t_1)\right\rangle. \tag{6}$$

The m wave mixing signal is given by a sum of 2^m terms, each factorized into a product of mth-order material and corresponding optical field SNGFs:

$$S_\alpha^{(m)}=\Im\frac{i^m2^{(m+1)/2}\delta_{m+1,\alpha}}{\pi m!\hbar^{m+1}}\sum_{\nu_m}\cdots\sum_{\nu_1}\int_{-\infty}^{\infty}\mathrm{d}t_{m+1}\,\mathrm{d}t_m\cdots\mathrm{d}t_1\times\Theta(t_{m+1})\mathbb{V}^{(m)}_{\nu_{m+1}\nu_m\ldots\nu_1}(t_{m+1},t_m,\ldots,t_1)\mathbb{E}^{(m)}_{\nu_{m+1}\bar{\nu}_m\ldots\bar{\nu}_1}\times(t_{m+1},t_m,\ldots,t_1), \tag{7}$$

where t_{m+1}, $t_m,\ldots,t_1$ are the light/matter interaction times. The factor $\Theta(t_{m+1})=\prod_{i=1}^{m}\theta(t_{m+1}-t_i)$ guarantees that the t_{m+1} is the last light–matter interaction. The indexes $\bar{\nu}_j$ are the conjugates to ν_j and are defined as follows: the conjugate of + is − and *vice versa*. Equation (7) implies that each material excitation is caused by fluctuations in the optical field and *vice versa*. The $2^{(m+1)/2}$ factor comes from the relation (A1) between the commutator (anti-commutator) and the superoperators.

Equation (7) also holds in the L,R representation, where the conjugate of 'left' is 'left' and the conjugate of 'right' is 'right': $\bar{L}=L,\bar{R}=R$. In this representation the coefficient $2^{(m+1)/2}$ must be replaced by unity. The material SNGFs,

$$\mathbb{V}^{(m)}_{\mathrm{L}\underbrace{L\ldots L}_{n}\underbrace{R\ldots R}_{m-n}},$$

represent a *Liouville space pathway* with $n+1$ interactions from the left (i.e. with the ket) and $m-n$ interactions from the right (i.e. with the bra).

We next recast the material SNGF (5) in the frequency domain by performing a multiple Fourier transform:

$$\chi^{(m)}_{\nu_{m+1}\nu_m\ldots\nu_1}(-\omega_{m+1};\omega_m,\ldots,\omega_1)=\int_{-\infty}^{\infty}\mathrm{d}t_{m+1}\ldots\mathrm{d}t_1\Theta(t_{m+1})\mathrm{e}^{i(\omega_mt_m+\cdots+\omega_1t_1)}\times\delta(-\omega_{m+1}+\omega_m+\cdots+\omega_1)\mathbb{V}^{(m)}_{\nu_{m+1}\nu_m\ldots\nu_1}\times(t_{m+1},t_m,\ldots,t_1). \tag{8}$$

The SNGF

$$\chi^{(m)}_{+\underbrace{-\cdots-}_{m}}(-\omega_{m+1};\omega_m,\ldots,\omega_1)$$

(with one + and the rest $m-$ indices) are the mth-order nonlinear susceptibilities derived from CRFs. Other SNGFs in the frequency domain with arbitrary combinations of + and − indices can be interpreted similarly to their time domain counterparts (5).

In the L,R representation, each material SNGF (8) represents a Liouville-space pathway. For some techniques it is more convenient to use a mixed representation of SNGF where some superoperators are in the L,R and others in the +, − representation.

In the following sections, the general formal expression for the signal (7) will be applied to calculate specific nonlinear techniques in a model molecular system by a proper choice of initial conditions for the optical field.

3. Heterodyne-detected sum and difference frequency generation

We first consider two second-order signals $S_3^{(2)}$ involving three classical modes. The third mode is singled out since it is heterodyne detected by measuring its time-averaged photon flux (number of photons per unit time).

The initial state of the field is given by a product of coherent states: $|t=-\infty\rangle=|\beta\rangle_1|\beta\rangle_2|\beta\rangle_3$, where $|\beta\rangle_\alpha$ are eigenfunctions of the mode α annihilation operator: $a_\alpha|\beta\rangle_\alpha=\beta_\alpha|\beta\rangle_\alpha$. Coherent states are the most classical quantum states of light [3].

For coherent optical states, all field SNGF in the L,R representation (6) are identical $E'_{\rm L}=E'_{\rm R}$ (the superoperator index makes no difference since all operations commute). In the +, − representation, no 'minus' indices are allowed, since $E'_{-}=0$. Only one type of optical SNGF then contributes to the classical signal:

$$\mathbb{E}^{(2)}_{+++}(t_3,t_2,t_1)=\mathcal{E}'(t_3)\mathcal{E}'(t_2)\mathcal{E}'(t_1), \tag{9}$$

where $\mathcal{E}'=\langle E'_{\rm L}\rangle=\langle E'_{\rm R}\rangle=\beta_\alpha\sqrt{2\pi\hbar\omega_\alpha/\Omega}$ is the classical field amplitude.

The conjugate material SNGFs (5) transformed into L, R representation contains eight terms, but only half of them are independent:

$$\begin{aligned}2^{3/2}\mathbb{V}^{(2)}_{+--}(t_3,t_2,t_1)=&\mathbb{V}^{(2)}_{\rm LLL}(t_3,t_2,t_1)-\mathbb{V}^{(2)}_{\rm LRL}(t_3,t_2,t_1)\\&-\mathbb{V}^{(2)}_{\rm LLR}(t_3,t_2,t_1)+\mathbb{V}^{(2)}_{\rm LRR}(t_3,t_2,t_1),\end{aligned} \tag{10}$$

where we have set the last interaction at the left branch.

To simplify Equation (10) further, we assume a three-level material scheme as shown in Figures 1(b) and 2(b). All transitions between the ground $|g\rangle$, intermediate $|e\rangle$ and $|f\rangle$ state manifolds are allowed. The dipole moment creation operator projected on mode α is given by

$$V^\dagger_\alpha=\mu^\alpha_{ge}|g\rangle\langle e|+\mu^\alpha_{ef}|e\rangle\langle f|+\mu^\alpha_{gf}|g\rangle\langle f|, \tag{11}$$

with the corresponding optical transition dipole moments $\mu^\alpha_{eg}=\mathbf{e}^\alpha\langle e|\mu|g\rangle$, $\mu^\alpha_{ef}=\mathbf{e}^\alpha\langle f|\mu|e\rangle$ and $\mu^\alpha_{gf}=\mathbf{e}^\alpha\langle f|\mu|g\rangle$. Initially, the material system is in the ground state $|g\rangle$. We further invoke the rotating-wave approximation (RWA) for the interaction Hamiltonian:

$$H_{\rm int}=-\sum_\alpha V^\dagger_\alpha E_\alpha(t)+\text{c.c.} \tag{12}$$

Without loss of generality we assume that the last interaction is emission. This implies that $\mathbb{V}^{(2)}_{\rm LRR}(t_3,t_2,t_1)=0$ since one can not de-excite the ground state.

In the RWA, the material SNGFs written in terms of L,R superoperators can be represented by the close-time path loop (CTPL) diagrams of the Schwinger–Keldysh many-body theory [8,9]. The rules for constructing these partially time-ordered diagrams are summarized in Appendix B. The complete set of CTPL diagrams corresponding to material SNGFs (10) are shown in Figures 1(c) and 2(c) (possible permutation of $\mathbf{k}_2$ and $\mathbf{k}_1$ is not shown). We shall show that the signals (7) are now given by the causal $\chi^{(2)}_{+--}(-\omega_3,\pm\omega_2,\pm\omega_1)$ response functions. This result is well known and can be obtained by using the standard semiclassical approach taking the optical fields to be classical. This calculation is given in order to illustrate how the SNGF formalism works.

To obtain nonlinear signals (7), the corresponding material SNGF (10) must be calculated for each technique by specifying the phase matching conditions (frequencies and wave vectors of the optical modes). This will be done below.

3.1. *Difference frequency generation (DFG)*

In DFG (Figure 1), the first mode $\mathbf{k}_1$ promotes the molecule from its ground state $|g\rangle$ into state $|f\rangle$, the second mode $\mathbf{k}_2$ induces stimulated emission from $|f\rangle$ to an intermediate $|e\rangle$ and the third mode $\mathbf{k}_3$ stimulates the emission from $|e\rangle$ to $|g\rangle$. All optical modes are linearly polarized in the $\mathbf{e}_x$ direction and the signal is measured in the phase matching direction $\mathbf{k}_3=\mathbf{k}_1-\mathbf{k}_2$.

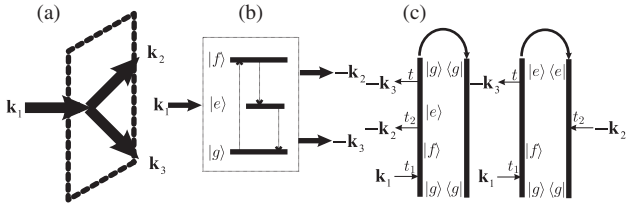

Figure 1. Heterodyne-detected DFG. (a) Phase-matching condition $\mathbf{k}_3=\mathbf{k}_1-\mathbf{k}_2$. (b) Molecular level scheme. (c) CTPL diagrams.

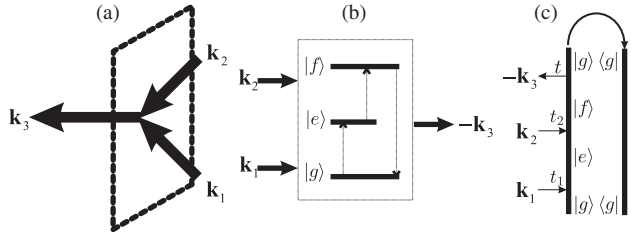

Figure 2. Heterodyne-detected SFG. (a) Phase-matching condition $\mathbf{k}_3=\mathbf{k}_1+\mathbf{k}_2$. (b) Level scheme. (c) CTPL diagrams.

The CTPL diagrams corresponding to this technique are shown in Figure 1(c).

The optical field SNGF in Equation (9) is

$$\mathbb{E}^{(2)}_{+++}(t_3,t_2,t_1)=\mathcal{E}^{\star}_3(t)\mathcal{E}^{\star}_2(t_2)\mathcal{E}_1(t_1). \tag{13}$$

The material SNGFs in Equation (10) become

$$\begin{aligned}2^{3/2}\mathbb{V}^{(2)}_{+--}(t_3,t_2,t_1)&=\langle \mathcal{T}V^3_{\mathrm{L}}(t_3)V^{2,\dagger}_{\mathrm{L}}(t_2)V^{1,\dagger}_{\mathrm{L}}(t_1)\\&\quad-\langle \mathcal{T}V^3_{\mathrm{L}}(t_3)V^{2,\dagger}_{\mathrm{R}}(t_2)V^{1,\dagger}_{\mathrm{L}}(t_1)\rangle\\&=\theta(t_2-t_1)\langle V^3(t_3)V^{2,\dagger}(t_2)V^{1,\dagger}(t_1)\\&\quad-\langle V^{1,\dagger}(t_1)V^3_{\mathrm{L}}(t_3)V^{2,\dagger}(t_2)\rangle.\end{aligned} \tag{14}$$

Note that $\mathbb{V}^{(2)}_{\mathrm{LLR}}(t_3,t_2,t_1)=0$ since the molecule cannot be de-excited from its ground state. The step function $\theta(t_2-t_1)$ indicates that interactions within one branch are time ordered.

Substituting (14) and (13) into (7), the DFG signal can be written in the frequency domain as

$$\begin{aligned}S_{\mathrm{DFG}}(-\omega_3,\omega_2,\omega_1)&=\frac{2^{3/2}}{\pi\hbar}\Im\mathcal{E}^{\star}_3\mathcal{E}^{\star}_2\mathcal{E}_1\chi^{(2)}_{+--}(-\omega_3;-\omega_2,\omega_1)\\&\quad\times\delta(\omega_1-\omega_2-\omega_3),\end{aligned} \tag{15}$$

where second-order susceptibility is give by

$$\begin{aligned}&2^{3/2}\chi^{(2)}_{+--}(-(\omega_1-\omega_2);-\omega_2,\omega_1)\\&=\frac{1}{2!\hbar^2}\Big(\Big\langle g|V_3G(\omega_g+\omega_1-\omega_2)V_2G(\omega_g+\omega_1)V^{\dagger}_1|g\Big\rangle\\&\quad-\Big\langle g|V_2G^{\dagger}(\omega_g+\omega_1-\omega_2)V_3G(\omega_g+\omega_1)V^{\dagger}_1|g\Big\rangle\Big).\end{aligned} \tag{16}$$

Here, $G(\omega)$ is the retarded Green's function,

$$G(\omega)=\frac{\hbar}{\hbar\omega-H_{\mathrm{mol}}+i\hbar\gamma}. \tag{17}$$

The advanced Green's function $G^{\dagger}(\omega)$ is its Hermitian conjugate and $\hbar\gamma$ is the dephasing rate. Note that the signal (16) can be directly obtained from the diagrams in Figure 1(c) simply by applying the rules given in Appendix B.

Expanding (17) in molecular eigenstates and substituting it into (16) gives

$$\begin{aligned}&2^{3/2}\chi^{(2)}_{+--}(-(\omega_1-\omega_2);-\omega_2,\omega_1)\\&=\frac{1}{2!\hbar^2}\frac{\mu^x_{gf}\mu^x_{fe}\mu^x_{eg}}{(\omega_1-\omega_{gf}+i\hbar\gamma_{gf})(\omega_1-\omega_2-\omega_{eg}+i\hbar\gamma_{eg})}\\&\quad-\frac{1}{2!\hbar^2}\frac{\mu^x_{gf}\mu^x_{fe}\mu^x_{eg}}{(\omega_1-\omega_{gf}+i\hbar\gamma_{gf})(\omega_2-\omega_{eg}-i\hbar\gamma_{eg})}.\end{aligned} \tag{18}$$

Equation (18) indicates that the signal induced by classical optical fields is given by the second-order CRF. This susceptibility tensor is used in the standard effective interaction Hamiltonian of quantum optics (44).

3.2. *Sum frequency generation SFG*

In SFG (Figure 2(a)) the first two modes promote the molecule from its ground state $|g\rangle$ through the intermediate state $|e\rangle$ into the final state $|f\rangle$. The third mode induces stimulated emission from $|f\rangle$ to the ground state $|g\rangle$. The signal is generated in the phase matching direction $\mathbf{k}_3=\mathbf{k}_1+\mathbf{k}_2$.

The heterodyne SFG signal can be obtained as we did for DFG, by utilizing diagram (c) of Figure 2:

$$\begin{aligned}S_{\mathrm{SFG}}(\omega_1,\omega_2)&=\frac{2^{3/2}}{\pi\hbar}\Im\mathcal{E}^{\star}_3\mathcal{E}_2\mathcal{E}_1\chi^{(2)}_{+--}(-\omega_3;\omega_2,\omega_1)\\&\quad\times\delta(\omega_1+\omega_2-\omega_3).\end{aligned} \tag{19}$$

The CRF is now given by

$$\begin{aligned}&2^{3/2}\chi^{(2)}_{+--}(-(\omega_1+\omega_2);\omega_2,\omega_1)\\&=\frac{1}{2!\hbar^2}\langle g|V_3G(\omega_g+\omega_1+\omega_2)V^{\dagger}_2G(\omega_g+\omega_1)V^{\dagger}_1|g\rangle\\&=\frac{1}{2!\hbar^2}\frac{\mu^x_{ge}\mu^x_{fe}\mu^x_{eg}}{(\omega_1-\omega_{eg}+i\hbar\gamma_{eg})(\omega_1+\omega_2-\omega_{gf}+i\hbar\gamma_{gf})}.\end{aligned} \tag{20}$$

SFG with three classical waves can be alternatively described in Hilbert space by an effective interaction Hamiltonian (43) with the material parameter given by Equation (20).

The purpose of this section was to illustrate how the superoperator approach works for well-known classical spectroscopic techniques. Since all the optical modes are classical (coherent states), the signal is given by the CRF. In the SNGFs language it can be translated into the second-order susceptibility $\chi^{(2)}_{+--}$. All moments of molecular fluctuations vanish identically ($\chi^{(2)}_{++-}=\chi^{(2)}_{+++}=0$). Starting from the $+,-$ representation we transformed the CRF into the L,R representation and employed the CTPL diagram technique to find the relevant molecular Liouville pathways and restore the signals.

In the following sections, Equations (20) and (18) will be compared with other techniques involving various combinations of quantum and classical optical fields. We shall apply the above algorithm in reverse order. That is, for each technique we identify the non-vanishing Liouville pathways in the L, R representation and then transform the signal into the $+$, $-$ representation. That representation reveals the role of the molecular fluctuations in the nonlinear signals.

4. Two-photon-induced fluorescence (TPIF) vs. homodyne SFG

We now turn to techniques involving two classical and one quantum mode where the initial state of the optical field is $|t=-\infty\rangle=|\beta_1\rangle_1|\beta_2\rangle_2|0\rangle_3$. We again assume the three-level material system (Figure 3(b)). We assume that the ground state is a manifold. By taking $\omega_{eg}\neq\omega_{ef}$ we focus on the resonant SNGFs and reduce the number of diagrams.

The two classical modes $\mathbf{k}_1$ and $\mathbf{k}_2$ promote the molecule from its ground state $|g\rangle$ through the intermediate state $|e\rangle$ into the final state $|f\rangle$. The system then spontaneously moves back into the ground state manifold $|g'\rangle$ by emitting a photon into the third detected mode $\mathbf{k}_3$, which is initially in the vacuum state (see Figure 3(b)).

The signal (photon flux in the $\mathbf{k}_3$ mode) involves three optical field modes and six light/matter interactions. Therefore, Equation (7) must by expanded to fifth order in $H_{\rm int}$. The fifth-order signal $S^{(5)}_{\rm CCQ}$ (CCQ denotes two classical and one quantum mode) may be written as a sum of 2^5 terms, each given by a product of molecule/field six-point SNGFs.

Only processes that satisfy the following conditions contribute to the signal.

(1) The creation operator of the quantum mode $a_3^\dagger$ must be accompanied by the corresponding annihilation operator a_3.
(2) The quantum mode can only de-excite the molecule (emission), which implies that the annihilation operator must act on the bra and the creation operator act on the ket.
(3) The coherent optical fields are tuned off-resonance with respect to the $\omega_{fg'}$ transition. Hence, the signal is not masked by stimulated emission.

We assume a collection of N non-interacting molecules positioned at $\mathbf{r}_i$ so that $V=\sum_i V_i\delta(\mathbf{r}-\mathbf{r}_i)$. The relevant CTPL diagrams for processes involving

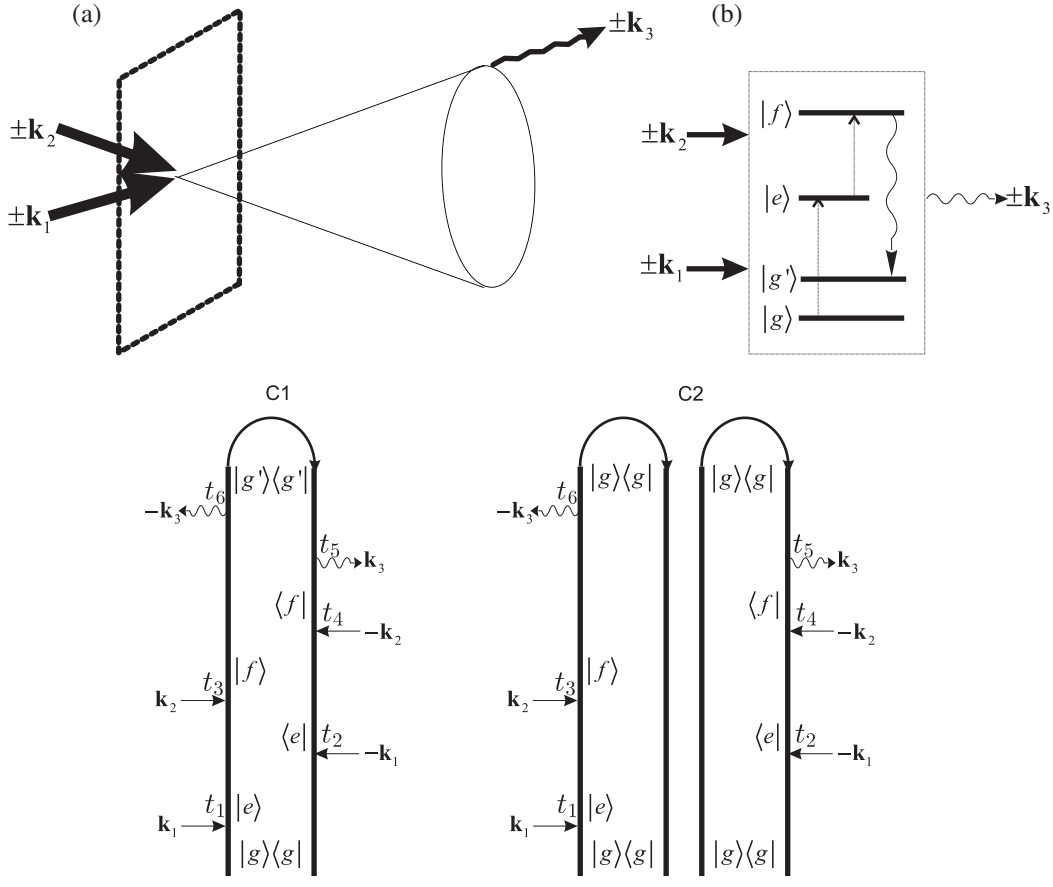

Figure 3. Three-wave process with two classical and one quantum mode (CCQ). (a) Phase-matching conditions: for TPIF the spontaneous mode is not particularly directed, but for the homodyne-detected SFG the mode is emitted into a cone determined by the reciprocal of the sample size. (b) Molecular level scheme. (C1) CTPL for the incoherent TPIF. (C2) Coherent homodyne-detected SFG. For the coherent signal, optical field interactions with molecule 1 of the pair occur from the left (L), and the interactions with molecule 2 occur form the right (R).

three optical modes and six light/matter interactions are presented in Figure 3(c). The field modes can either interact with the same molecule (incoherent process, Figure 3(C1)) or with two different molecules (coherent process, Figure 3(C2)) [8].

4.1. *Two-photon-induced fluorescence (TPIF)*

TPIF is an incoherent three-wave process involving two classical and one quantum mode. The phase-matching condition $\mathbf{k}_1-\mathbf{k}_1+\mathbf{k}_2-\mathbf{k}_2+\mathbf{k}_3-\mathbf{k}_3=0$ is automatically satisfied for any $\mathbf{k}_3$. The actual angular distribution of the spontaneously emitted photons is determined by Equation (26) and the electric field vectors of the input, subject to rotational diffusion over the two-photon excited-state lifetime. Using the identity $\sum_{i=1}^{N}\exp i(\mathbf{k}_1-\mathbf{k}_1+\mathbf{k}_2-\mathbf{k}_2+\mathbf{k}_3-\mathbf{k}_3)\times(\mathbf{r}-\mathbf{r}_i)=N$ we obtain the optical field SNGF (6):

$$\mathbb{E}^{(5)}_{\mathrm{LR}++++}(t_6,t_5,\ldots,t_1) = N\mathcal{E}_1(t_1)\mathcal{E}_1^{\star}(t_2)\mathcal{E}_2(t_3)\mathcal{E}_2^{\star}(t_4)\frac{2\pi\hbar\omega_3}{\Omega}\exp\left(i\omega_3(t_6-t_5)\right). \tag{21}$$

The relevant material SNGF (5) is

$$\mathbb{V}^{(5)}_{\mathrm{LR}----}(t_6,t_5,\ldots,t_1) = \langle\mathcal{T}V^{3}_{\mathrm{L}}(t_6)V^{3,\dagger}_{\mathrm{R}}(t_5)V^{2}_{-}(t_4)V^{2,\dagger}_{-}(t_3)V^{1}_{-}(t_2)V^{1,\dagger}_{-}(t_1)\rangle. \tag{22}$$

Utilizing Equations (21) and (22), the frequency domain signal can be written as

$$S_{\mathrm{TPIF}}(\omega_1,\omega_2)=\frac{N}{\pi\hbar}\sum_{\mathbf{k}_3}|\mathcal{E}_1|^2|\mathcal{E}_2|^2\frac{8\pi\hbar\omega_3}{\Omega}\Im\chi^{(5)}_{\mathrm{LR}----}\times(-\omega_3;\omega_3,-\omega_2,\omega_2,-\omega_1,\omega_1). \tag{23}$$

Note that the above expression is given in the mixed (L/R, +/−) representation. It can be transformed into the +, − representation using the identity

$$2\chi^{(5)}_{\mathrm{LR}----}=\chi^{(5)}_{++----}-\chi^{(5)}_{+--+--}. \tag{24}$$

Here, the first term (two 'plus' four 'minus' indices) arises since one of the modes is not classical. The second term is the ordinary CRF.

The material SNGF in the frequency domain (8) can be calculated by switching to the L, R representation:

$$\chi^{(5)}_{\mathrm{LR}----}(-\omega_3;\omega_3,-\omega_2,\omega_2,-\omega_1,\omega_1)=\frac{1}{4}\chi^{(5)}_{\mathrm{LRLRLR}}(-\omega_3;\omega_3,-\omega_2,\omega_2,-\omega_1,\omega_1),$$

and utilizing diagram (C1) of Figure 3:

$$\chi^{(5)}_{\mathrm{LRLRLR}}(-\omega_3;\omega_3,-\omega_2,\omega_2,-\omega_1,\omega_1) = \frac{1}{5!\hbar^5}\langle g|V_1G^{\dagger}(\omega_g+\omega_1)V_2G^{\dagger}(\omega_g+\omega_1+\omega_2) \times V_3^{\dagger}G^{\dagger}(\omega_g+\omega_1+\omega_2-\omega_3) \times V_3G(\omega_g+\omega_1+\omega_2)V_2^{\dagger}G(\omega_g+\omega_1)V_1^{\dagger}|g\rangle. \tag{25}$$

Expanding Equation (25) in molecular states gives

$$4\chi^{(5)}_{\mathrm{LR}----}(-(\omega_1+\omega_2);\omega_2,\omega_1) = \sum_{gg'}|\mu^{x}_{g'f}\mu^{x}_{fe}\mu^{x}_{eg}|^2 \times\frac{1}{5!\hbar^5}\frac{1}{[(\omega_1-\omega_{eg})^2+\gamma^2_{eg}][\omega_1+\omega_2-\omega_{fg}+i\gamma_{fg}]} \times\frac{1}{[\omega_1+\omega_2-\omega_{fg'}-i\gamma_{fg'}][\omega_1+\omega_2-\omega_3-\omega_{gg'}-i\gamma_{gg'}]}. \tag{26}$$

Provided the energy splitting within the ground state manifold $\omega_{gg'}$ is small compared with the optical transitions, the signal can be recast in the form

$$S_{\mathrm{TPIF}}(\omega_1,\omega_2)=\frac{2N\omega_3}{5!\hbar^5\Omega}|\mathcal{E}_1|^2|\mathcal{E}_2|^2|T_{g'g}(\omega_1,\omega_2)|^2 \times\delta(\omega_1+\omega_2-\omega_3-\omega_{gg'}), \tag{27}$$

with the transition amplitude

$$T_{g'g}(\omega_1,\omega_2)=\frac{\mu_{g'f}\mu_{fe}\mu_{eg}}{(\omega_1-\omega_{eg}+i\gamma_{eg})(\omega_1+\omega_2-\omega_{fg}+i\gamma_{fg})}.$$

This is a direct generalization of the Kramers–Heisenberg form of ordinary (single-photon) fluorescence [4,8].

The SNGF in Equation (25) has been referred to as the fluorescence quantum efficiency by Webb [19] or the two-photon tensor by Callis [20]. Our result is identical to that of Callis.

When the two classical coherent modes are degenerate ($\omega_1=\omega_2$) the signal in Equation (27) describes non-resonant hyper-Raman scattering ($\omega_{gg'}\neq 0$), also known as incoherent second harmonic inelastic scattering [20,23,24]. When $\omega_1=\omega_2$ and $\omega_{gg'}\to 0$ (but not equal to), Equation (27) describes off-resonant hyper-Rayleigh scattering, also known as incoherent second harmonic elastic scattering. Off-resonant hyper-scattering is a major complicating factor for TPIF microscopy [25]. The distinction between hyper-Raman and TPIF processes is analogous to their single-photon counterparts (ordinary Raman and fluorescence) as shown in Ref. [4]. The difference between the two can be clarified by

adding pure dephasing processes. This goes beyond the present CTPL treatment.

4.2. *Homodyne-detected sum frequency generation*

The coherent part of the $S^{(5)}_{\mathrm{CCQ}}$ signal ((C2) in Figure 3) describes homodyne-detected SFG. Photons in the $\mathbf{k}_3$ mode are spontaneously emitted into a cone [1] of solid angle $\sim\Delta\mathbf{k}$. Here the phase matching $\Delta\mathbf{k}\approx\mathbf{k}_1+\mathbf{k}_2-\mathbf{k}_3$ reflects the uncertainty in the phase given by the reciprocal of the sample characteristic size. For a large sample, one can assume $\Delta\mathbf{k}\approx 0$, which effectively narrows the optical cone. The optical field SNGF is given by Equation (21), but the factor N it now replaced by

$$\sum_{i=1}^{N}\sum_{j\neq i}^{N-1} e^{i\Delta\mathbf{k}(\mathbf{r}-\mathbf{r}_i)}e^{-i\Delta\mathbf{k}(\mathbf{r}-\mathbf{r}_j)}\approx N(N-1). \tag{28}$$

For large N the coherent part $\sim N(N-1)$ dominates over the incoherent $\sim N$ response. For a small sample size, exact calculation of the optical field part of the SNGF is rather lengthy, but can be performed in the same fashion as done by Hong and Mandel [13] for the probability of photon detection.

We next turn to the material SNGF. For the coherent process we must work in the joint space of two molecules $|\rangle_{1,2}=|\rangle_1|\rangle_2$ interacting with the same field mode. Hence, the material SNGF of the joint system can be factorized into a product of SNGF of molecule 1 and 2:

$$\begin{aligned}&\mathbb{V}^{(5)}_{\mathrm{LR}----}(t_6,t_5,\ldots,t_1)\\&=\left\langle \mathcal{T}V^3_+(t_6)V^{3,\dagger}_+(t_5)V^2_-(t_4)V^{2,\dagger}_-(t_3)V^1_-(t_2)V^{1,\dagger}_-(t_1)\right\rangle\\&=\left\langle \mathcal{T}V^3_+(t_6)V^{2,\dagger}_-(t_3)V^{1,\dagger}_-(t_1)\rangle_1\langle\mathcal{T}V^{3,\dagger}_+(t_5)V^2_-(t_4)V^1_-(t_2)\right\rangle_2,\end{aligned} \tag{29}$$

where we have used the fact that the last interaction must be a 'plus' and the field interactions with the two molecules are not time ordered.

Using Equation (29) the coherent material SNGF in the frequency domain assumes the form of the square of a second-order CRF:

$$\begin{aligned}&2^{6/2}\Im\chi^{(5)}_{++----}(-\omega_3;\omega_3,-\omega_2,\omega_2,-\omega_1,\omega_1)\\&\quad=|2^{3/2}\chi^{(2)}_{+--}(-(\omega_1+\omega_2);\omega_2,\omega_1)\|^2.\end{aligned}$$

This result can also be obtained in the L, R representation using diagram (C2) in Figure 3. The classical modes excite the molecules and the quantum mode de-excites them. Hence, the interactions with the first molecule ket (L) are accompanied by the conjugate interactions with the second molecule bra (R). Transforming the first molecule diagram into the $+,-$ representation we find that the first molecule contributes the causal response $\chi^{(2)}_{\mathrm{LLL}}(-(\omega_1+\omega_2);\omega_2,\omega_1)=2^{3/2}\chi^{(2)}_{+--}(-(\omega_1+\omega_2);\omega_2,\omega_1)$ given by Equation (20). The second molecule provides the conjugate causal response.

The homodyne-detected SFG signal is finally given by

$$\begin{aligned}S_{\mathrm{SFG}}=N(N-1)|\mathcal{E}_1|^2|\mathcal{E}_2|^2\frac{2(\omega_1+\omega_2)}{\Omega}|2^{3/2}\chi^{(2)}_{+--}\\\times(-(\omega_1+\omega_2);\omega_2,\omega_1)|^2.\end{aligned} \tag{30}$$

Equation (30) can alternatively be obtained from the effective interaction Hamiltonian of the form (43), where the material parameter is given by the causal response function $\chi^{(2)}_{+--}(-(\omega_1+\omega_2);\omega_2,\omega_1)$.

Both homodyne and heterodyne SFG are given by the same CRF $\chi^{(2)}_{+--}$. The main difference is that the latter process satisfies the perfect phase-matching condition, while for the former this condition is only approximate and becomes exact for sufficiently large samples.

To summarize this section we give the total signal for a three-wave process involving two classical and one quantum field (CCQ) which includes both the incoherent and coherent components:

$$\begin{aligned}S^{(5)}_{\mathrm{CCQ}}(\omega_2,\omega_1)=|\mathcal{E}_1|^2|\mathcal{E}_2|^2\frac{2\omega_3}{\Omega}\Big[N2^{6/2}\Im\chi^{(5)}_{++----}\\\times(-\omega_3;\omega_3,-\omega_2,\omega_2,-\omega_1,\omega_1)\\-N2^{6/2}\Im\chi^{(5)}_{+-----}\\\times(-\omega_3;\omega_3,-\omega_2,\omega_2,-\omega_1,\omega_1)\\+N(N-1)|2^{3/2}\delta(\omega_3-\omega_1-\omega_2)\\\times\chi^{(2)}_{+--}(-\omega_3;\omega_2,\omega_1)|^2\Big].\end{aligned} \tag{31}$$

5. Two-photon-emitted fluorescence (TPEF) vs. Type I parametric down conversion (PDC)

We now turn to three-wave processes involving one classical and two quantum modes (Figure 4). We start with the incoherent response of N identical molecules initially in their ground state and the initial state of the optical field is $|t=-\infty\rangle=|\beta_1\rangle_1|0\rangle_2|0\rangle_3$. The classical field $\mathbf{k}_1$ pumps the molecule from its ground state $|g\rangle$ into the excited state $|f\rangle$. The system then spontaneously emits two photons into modes $\mathbf{k}_2$ and $\mathbf{k}_3$ (see Figure 4(b)) which are initially in the vacuum state. This incoherent process which involves one classical

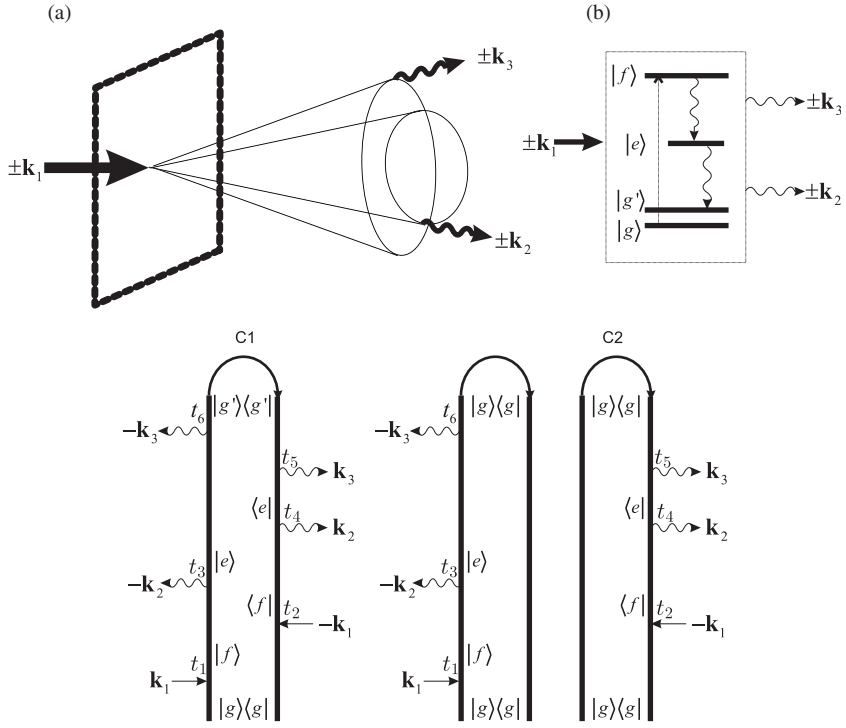

Figure 4. Three-wave process with two quantum and one classical modes (QQC). (a) Phase-matching conditions: for TPEF, spontaneous modes are not directed, but for PDC the modes are emitted into two collinear cones. (b) Molecular level scheme. CTPL for the incoherent TPEF (C1) and coherent Type I PDC (C2). In panel (C2), the two diagrams correspond to the conjugate pathways of the molecules in the pair.

and two quantum modes will be denoted as two-photon-emitted fluorescence (TPEF). It is phase-insensitive since the phase-matching condition $\mathbf{k}_1 - \mathbf{k}_1 + \mathbf{k}_2 - \mathbf{k}_2 + \mathbf{k}_3 - \mathbf{k}_3 = 0$ is automatically satisfied for any $\mathbf{k}_3$. To facilitate the subsequent comparison with Type I parametric down conversion (PDC), we adopted the following beam polarization configuration as is usually done for PDC of this type: the spontaneously generated photons are polarized along the x axis, and the classical mode polarized along the y axis.

The TPEF signal is given by the time-averaged photon flux in the $\mathbf{k}_3$ mode. We again make use of the CTPL diagrams to find the relevant SNGF given the initial state of the field; the diagrams must satisfy the following conditions.

(1) Creation operators of the spontaneously generated modes $a_3^\dagger$ and $a_2^\dagger$ acting on the ket must be accompanied by corresponding annihilation operators a_3 and a_2 acting on the bra.
(2) The first mode $\omega_1(\mathbf{k}_1)$ is off-resonance with respect to both ω_{eg} and ω_{fe} transitions. Stimulated emission can thus be neglected.
(3) The spontaneous modes have different frequencies; modes $\mathbf{k}_2$ and $\mathbf{k}_3$ are resonant with ω_{fe} and ω_{eg}, respectively.

These conditions are satisfied by diagram (C1) in Figure 4. The non-resonant diagrams have been omitted. Using this diagram we obtain the following optical field and material SNGFs:

$$\mathbb{E}^{(5)}_{\mathrm{LLRR}++}t(t_6,t_5,\ldots,t_1) = N\mathcal{E}_1(t_1)\mathcal{E}_1^{\star}(t_2)\frac{2\pi\hbar\omega_3}{\Omega}\frac{2\pi\hbar\omega_2}{\Omega}\exp\left(i\omega_3(t_6-t_5)\right) \times \exp\left(i\omega_3(t_4-t_3)\right), \quad (32)$$

$$\mathbb{V}^{(5)}_{\mathrm{LLRR}--}(t_6,t_5,\ldots,t_1) = \left\langle \mathcal{T} V_{\mathrm{L}}^{3}(t_6)V_{\mathrm{R}}^{3,\dagger}(t_5)V_{\mathrm{R}}^{2,\dagger}(t_4)V_{\mathrm{L}}^{2}(t_3)V_{-}^{1}(t_2)V_{-}^{1,\dagger}(t_1)\right\rangle. \quad (33)$$

Using Equations (32) and (33) the incoherent part of the signal in the frequency domain is given by

$$S_{\mathrm{TPEF}}(\omega_1) = \frac{N}{\pi\hbar}|\mathcal{E}_1|^2\frac{2\pi\hbar(\omega_2)}{\Omega}\frac{2\pi\hbar\omega_3}{\Omega}\Im 2\chi^{(5)}_{\mathrm{LRLR}--} \times(-\omega_3;\omega_3,-\omega_2,\omega_2,\omega_1,-\omega_1).$$

The corresponding SNGF can be calculated using diagram (C1) in Figure 4:

$$
\begin{aligned}
&-2\chi^{(5)}_{\mathrm{LRLR}--}(-\omega_3;\omega_3,-\omega_2,\omega_2,\omega_1,-\omega_1)\\
&\quad=\chi^{(5)}_{\mathrm{LRLRLR}}(-\omega_3;\omega_3,-\omega_2,\omega_2,\omega_1,-\omega_1)\\
&\quad=\frac{1}{5!\hbar^5}\Big\langle g|V_1^{\dagger}G^{\dagger}(\omega_g+\omega_1)V_2^{\dagger}G^{\dagger}(\omega_g+\omega_1-\omega_2)\\
&\qquad\times V_3G^{\dagger}(\omega_g+\omega_1-\omega_2-\omega_3)V_3G(\omega_g+\omega_1-\omega_2)\\
&\qquad\times V_2G(\omega_g+\omega_1)V_1^{\dagger}|g\Big\rangle.
\end{aligned}
$$

Expansion in the molecular eigenstates gives the frequency-domain response function in the Kramers–Heisenberg form:

$$
\begin{aligned}
&-2\chi^{(5)}_{\mathrm{LRLR}--}(-\omega_3;\omega_3,-\omega_2,\omega_2,\omega_1,-\omega_1)\\
&\quad=\frac{1}{5!\hbar^5}\sum_{gg'}\left|\mu^x_{g'e}\mu^x_{ef}\mu^y_{fg}\right|^2\frac{1}{(\omega_1-\omega_{fg})^2+\gamma_{fg}^2}\\
&\qquad\times\left|\frac{1}{\omega_1-\omega_2-\omega_{eg}+i\gamma_{eg}}\right|^2\delta(\omega_1-\omega_2-\omega_3).
\end{aligned}
\tag{34}
$$

Equation (34) can be recast in the L,R and +, − representations:

$$
\begin{aligned}
&\chi^{(5)}_{\mathrm{LRLR}--}(-\omega_3;\omega_3,-\omega_2,\omega_2,\omega_1,-\omega_1)\\
&\quad=-\frac{1}{4}\chi^{(5)}_{++----}(-\omega_3;\omega_3,-\omega_2,\omega_2,\omega_1,-\omega_1)\\
&\qquad-\frac{1}{4}\chi^{(5)}_{+++---}(-\omega_3;\omega_3,-\omega_2,\omega_2,\omega_1,-\omega_1)\\
&\qquad+\frac{1}{4}\chi^{(5)}_{++-+--}(-\omega_3;\omega_3,-\omega_2,\omega_2,\omega_1,-\omega_1)\\
&\qquad+\frac{1}{4}\chi^{(5)}_{+++++--}(-\omega_3;\omega_3,-\omega_2,\omega_2,\omega_1,-\omega_1).
\end{aligned}
$$

Unlike TPIF, the TPEF signal does not depend on the CRF $\chi^{(5)}_{+-----}$. The TPEF is solely determined by the various moments of the molecular fluctuations which are represented by other types of response function.

5.1. *Type I PDC*

We now turn to the coherent response from a collection of identical molecules which interact with one classical pumping mode to spontaneously generate two quantum modes (see Figure 4(a) and (b)) with the same polarization. This Type I parametric down conversion (PDC) process is widely used for producing entangled photon pairs. Spontaneously generated modes are emitted into two collinear cones, as shown in Figure 4(a). Hereafter, we assume perfect phase matching $\Delta\mathbf{k}=\mathbf{k}_1-\mathbf{k}_2-\mathbf{k}_3$ which is the case for sufficiently large samples [1].

The initial conditions for PDC are the same as for TPEF and most PDC experiments are well described by the CRF $\chi^{(2)}_{+--}$. Therefore, one would expect a connection between TPEF and PDC, similar to that of TPIF and homodyne-detected SFG. However, as we are about to demonstrate, the causal second-order response function does not provide a complete description of the PDC process.

To compute corrections to the second-order CRF caused by the quantum origin of the spontaneous modes we again resort to the CTPL diagrams (see Figure 4(C2)). For the coherent response from the molecular pairs, the optical field SNGF is given by Equation (32) with the factor N replaced by $N(N-1)$. The material SNGF (33) can be factorized into the product of conjugate SNGFs for the first and second molecule of the pair, as shown in Figure 4(C2):

$$
\begin{aligned}
&2\mathbb{V}^{(5)}_{\mathrm{LLRR}--}(t_6,t_5,\ldots,t_1)\\
&\quad=\left\langle\mathcal{T}V^3_{\mathrm{L}}(t_6)V^2_{\mathrm{L}}(t_3)V^{1,\dagger}_{\mathrm{L}}(t_1)\right\rangle_1\left\langle\mathcal{T}V^{3,\dagger}_{\mathrm{R}}(t_5)V^{2,\dagger}_{\mathrm{R}}(t_4)V^1_{\mathrm{R}}(t_2)\right\rangle_2.
\end{aligned}
\tag{35}
$$

Note that this factorization is unique since $\langle\mathcal{T}V^3_{\mathrm{L}}(t_6)V^{2,\dagger}_{\mathrm{R}}(t_4)V^{1,\dagger}_{\mathrm{L}}(t_1)\rangle=0$ when the material is initially in its ground state. Using this factorization the coherent PDC signal in the frequency domain can be written as

$$
\begin{aligned}
S_{\mathrm{PDC}}(\omega_1,\omega_2)=&\frac{N(N-1)}{4\pi\hbar}|\mathcal{E}_1|^2\frac{2\pi\hbar\omega_2}{\Omega}\frac{2\pi\hbar(\omega_1-\omega_2)}{\Omega}\\
&\times\left|2^{1/2}\chi^{(2)}_{\mathrm{LL}-}(-(\omega_1-\omega_2);-\omega_2,\omega_1)\right|^2.
\end{aligned}
\tag{36}
$$

Here, the generalized response function expanded in the eigenstates assumes the form

$$
\begin{aligned}
&2^{1/2}\chi^{(2)}_{\mathrm{LL}-}(-(\omega_1-\omega_2);-\omega_2,\omega_1)\\
&\quad=\chi^{(2)}_{\mathrm{LLL}}(-(\omega_1-\omega_2);-\omega_2,\omega_1)\\
&\quad=\frac{1}{2!\hbar^2}\frac{\mu^y_{gf}\mu^x_{fe}\mu^x_{eg}}{(\omega_1-\omega_{gf}+i\hbar\gamma_{gf})(\omega_1-\omega_2-\omega_{eg}+i\hbar\gamma_{eg})}.
\end{aligned}
$$

This mixed representation can be transformed into the +, − representation

$$
\chi^{(2)}_{\mathrm{LL}-}=\tfrac{1}{2}(\chi^{(2)}_{+--}+\chi^{(2)}_{++-}).
\tag{37}
$$

Comparing the CRF for heterodyne-detected DFG (18) and the SNGFs for Type I PDC (37) we see that the latter is described not only by CRF $\chi^{(2)}_{+--}$ but also by the second moment of material fluctuations $\chi^{(2)}_{++-}$. In the L,R representation it selects one Liouville pathway $\chi^{(2)}_{\mathrm{LLL}}$, while the classical optical fields drive the material system along all possible pathways.

The SNGF formalism suggests that Type I PDC can be calculated by using the effective interaction Hamiltonian (44) with the material parameter $\chi^{(2)} = \chi^{(2)}_{\mathrm{LLL}}(-(\omega_1 - \omega_2); -\omega_2, \omega_1)$.

In concluding this section we give the signal for the three-wave process involving one classical and two quantum fields (CQQ) which contains both an incoherent and a coherent component:

$$S^{(5)}_{\mathrm{CQQ}}(\omega_2, \omega_1) = \frac{1}{\pi\hbar}|\mathcal{E}_1|^2 \frac{2\pi\hbar\omega_2}{\Omega}\frac{2\pi\hbar\omega_3}{\Omega} N\Im 2\chi^{(5)}_{\mathrm{LRLR}--} \times (-\omega_3; \omega_3, -\omega_2, \omega_2, \omega_1, -\omega_1) + N(N-1)|2^{1/2}\delta(\omega_3 + \omega_2 - \omega_1)\chi^{(2)}_{\mathrm{LL}-} \times (-\omega_3; -\omega_2, \omega_1)|^2. \quad (38)$$

6. Type II PDC; polarization entanglement

In Type II parametric down-conversion, the two spontaneously generated photons have orthogonal polarizations. Because of birefringence, the photons are emitted along two non-collinear spatial cones known as ordinary and extraordinary beams (see Figure 5(a)). Polarization-entangled light [1,26] is generated at the intersections of these cones. An x polarization filter and a detector are placed at one of the cone intersections. The detector cannot tell from which beam a given photon originates. The process involves five optical modes: one classical $|1\rangle|y\rangle$ and four quantum modes $\{|2\rangle|x\rangle, |2\rangle|y\rangle, |3\rangle|x\rangle, |3\rangle|y\rangle\}$.

The polarization-entangled signal is described by the CTPL diagrams shown in Figure 5(c). The Type II PDC signal has two contributions $S^{(5)}_{\mathrm{PDCII}} = S^{(5)}_{3x} + S^{(5)}_{2x}$. The signal $S^{(5)}_{3x}$ assumes the form of Equation (36), with the material pathway depicted in Figure 5(C1):

$$\chi^{(2)}_{\mathrm{LL}-}(-(\omega_1 - \omega_2); -\omega_2, \omega_1) = \frac{1}{2}\left[\chi^{(2)}_{+--}(-(\omega_1 - \omega_2); -\omega_2, \omega_1) + \chi^{(2)}_{++-} \times (-(\omega_1 - \omega_2); \omega_2, -\omega_1)\right] = \frac{1}{2!\hbar^2}\frac{C}{(\omega_1 - \omega_{gf} + i\hbar\gamma_{gf})(\omega_1 - \omega_2 - \omega_{eg} + i\hbar\gamma_{eg})}, \quad (39)$$

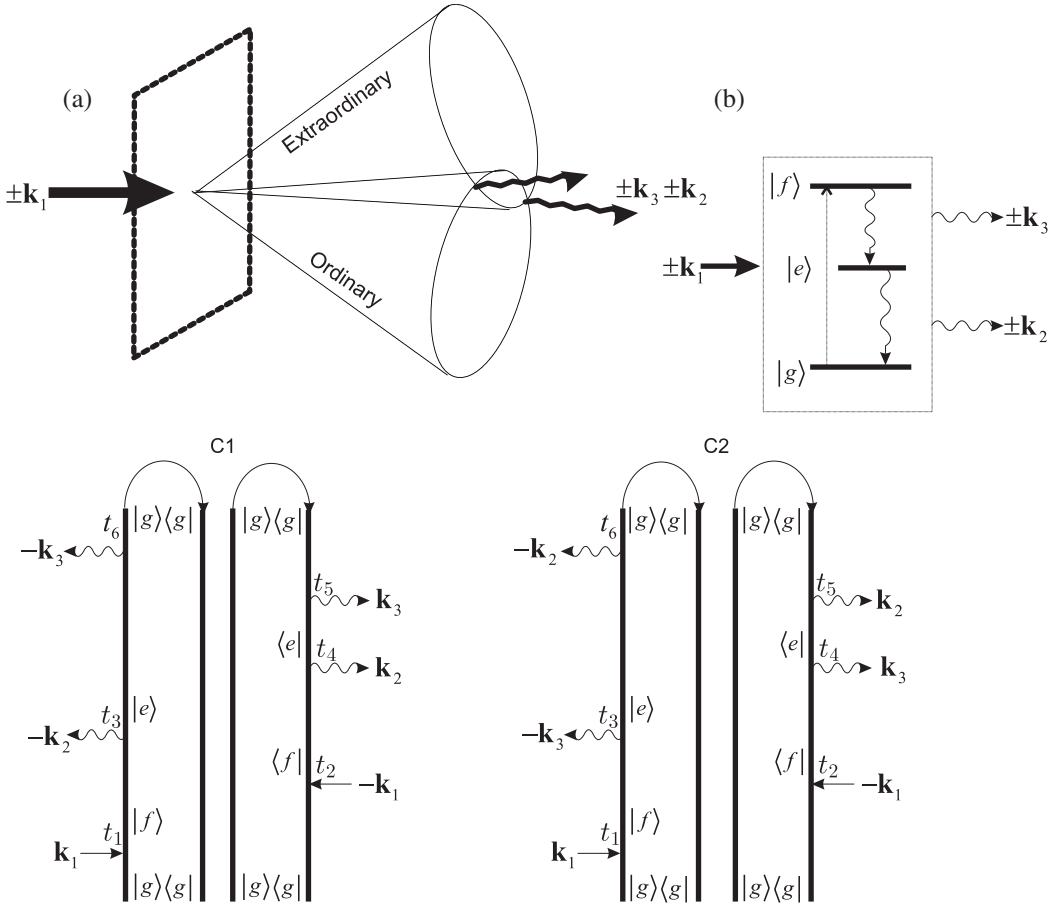

Figure 5. Type II PDC. (a) Phase matching. (b) Molecular level scheme. (c) CTPL diagrams for the coherent signal from $\mathbf{k}_3$ (C1) and $\mathbf{k}_2$ (C2) modes polarized along the x direction.

where the coefficient C is given by

$$C^2 = |\mu^y_{gf}|^2\Big(|\mu^x_{fe}|^2|\mu^x_{eg}|^2 + 2\mu^x_{fe}\mu^x_{eg}\mu^y_{fe}\mu^y_{eg} + \mu^x_{fe}\mu^x_{eg}\mu^x_{fe}\mu^y_{eg} + \mu^y_{fe}\mu^y_{eg}\mu^y_{fe}\mu^x_{eg}\Big). \quad (40)$$

The signal $S^{(5)}_{3x}$ is described by diagrams (C2) in Figure 5:

$$\begin{aligned}\chi^{(2)}_{\mathrm{LL}-}(-\omega_2;-(\omega_1-\omega_2),\omega_1) &= \frac{1}{2}\Big(\chi^{(2)}_{+--}(-\omega_2;-(\omega_1-\omega_2),\omega_1\Big) + \chi^{(2)}_{++-} \\ &\quad\times(-\omega_2;-(\omega_1-\omega_2),\omega_1)) \\ &= \frac{1}{2!\hbar^2}\frac{C}{(\omega_1-\omega_{gf}+i\hbar\gamma_{gf})(\omega_2-\omega_{eg}+i\hbar\gamma_{eg})}. \end{aligned} \quad (41)$$

The total Type II PDC signal is

$$\begin{aligned}S_{\mathrm{PDCII}}(\omega_1) = \frac{N(N-1)}{4\pi\hbar}|\mathcal{E}_1|^2\frac{2\pi\hbar\omega_2}{\Omega}\frac{2\pi\hbar(\omega_1-\omega_2)}{\Omega} \\ \times\Big[\Big|2^{1/2}\chi^{(2)}_{\mathrm{LL}-}(-(\omega_1-\omega_2);-\omega_2,\omega_1)\Big|^2 \\ +\Big|2^{1/2}\chi^{(2)}_{\mathrm{LL}-}(-\omega_2;-(\omega_1-\omega_2),\omega_1)\Big|^2\Big]. \end{aligned} \quad (42)$$

In Figure 6, we compare the generalized response given by the SNGFs $(\chi^{(2)}_{+--}+\chi^{(2)}_{++-})/2$ in Equation (41) with the CRF $\chi^{(2)}_{+--}$ (see Equation (18)) commonly used to describe both types of PDC. We assume a model material system with the following parameters. The transition dipole moments are $\mu^y_{gf}=\mu^x_{fe}=\mu^x_{eg}=0.1$ and $\mu^y_{eg}=\mu^y_{fe}=0$ (arbitrary units). For all transitions the dephasing rates are the same $\hbar\gamma_{gf}=\hbar\gamma_{eg}=0.05\omega_{gf}$. The classical mode $\mathbf{k}_1$ provides a common factor for the causal and generalized response function:

$$\frac{|\mu_{gf}|^2}{\omega_1-\omega_{gf}+i\hbar\gamma_{fg}}.$$

Hence, we can assume it to be in resonance with the $\omega_1\approx\omega_{gf}$ transition.

In Type II PDC the SNGF approach and conventional CRF description give quantitatively similar results as both resonances ($\omega_2\approx\omega_{eg}$ and $\omega_1-\omega_2\approx\omega_{eg}$) participate (Figure 6(a)). On the other hand, Type I PDC has only one resonance in the SNGF $\omega_1-\omega_2\approx\omega_{eg}$ and, therefore, is qualitatively different from the CRF near the resonance (Figure 6(b)). The off-resonant regime is well described by the CRF.

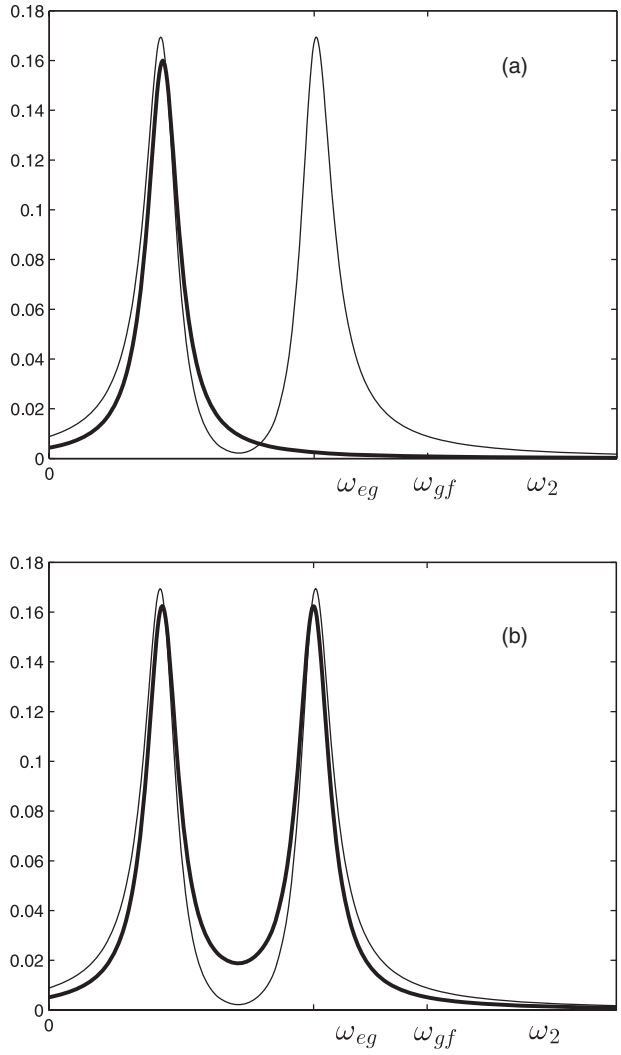

Figure 6. (a) The Type I PDC signal (36) is given by the SNGF (thick solid line) and by the standard causal response function (thin solid curve). (b) Type II PDC signal (42) given by the SNGFs (thick solid line) is compared with the signal given by the causal response function (thin solid curve). Perfect matching conditions are assumed and the classical beam frequency is set in resonance with ω_{gf} (for parameters, see text). The signal dependence on ω_2 is shown.

7. Conclusions

In quantum optics, a three-wave mixing process is commonly described by an effective interaction Hamiltonian for radiation modes [12]. For SFG this reads

$$H_{\mathrm{eff}} = -\int \mathrm{d}\mathbf{r}\,\chi^{(2)}E^{\dagger}_3(\omega_1-\omega_2)E^{\dagger}_2(\omega_2)E_1(\omega_1), \quad (43)$$

and for DFG and PDC

$$H_{\mathrm{eff}} = -\int \mathrm{d}\mathbf{r}\,\chi^{(2)}E^{\dagger}_3(\omega_1+\omega_2)E_2(\omega_2)E_1(\omega_1). \quad (44)$$

In both cases, the second-order nonlinearity tensor $\chi^{(2)}$ is responsible for the coupling between the modes.

The various techniques differ in the initial state of the fields. The nonlinearity tensor is given by the second-order susceptibility $\chi^{(2)}_{+--}$. This is based on the assumption that the molecular response is classical: it is described by the causal response function (CRF) and optical fields are not affected by material fluctuations. This assumption is justified only when *all* optical modes are in coherent classical states; adding (subtracting) a single photon to such modes has no noticeable effect.

Here we consider techniques that also involve optical modes initially in the vacuum state. The changes in their state due to material fluctuations must then be taken into account and these processes may not be described by the conventional causal response function. The parametric model (Equations (43) and (44)) must be modified to incorporate non-causality by treating both light and matter quantum mechanically.

A unified framework for calculating nonlinear optical signals generated in a material system by interactions with any combination of quantum and classical radiation fields is provided by the SNGF formalism developed in this article. When the optical fields are in coherent states the SNGFs reduce to the CRF, as demonstrated here for heterodyne-detected SFG and DFG techniques. The CRF contains all possible molecular Liouville pathways. In the SNGF formalism this is seen by switching from the $+$, $-$ to the L,R representations of the SNGFs. When quantum optical fields are involved, the number of available pathways may be reduced. At the same time, various moments of molecular fluctuations play an essential role in the nonlinear signal. Here this is shown by switching from the L,R to the $+$, $-$ representation. Several spectroscopic techniques that involve both quantum and classical optical fields were considered.

We have examined the applicability of the conventional second-order parametric model for the description of the PDC and homodyne-detected SFG, since the processes involve highly non-classical spontaneously generated modes. We compared the incoherent TPEF and the coherent PDC signals. The incoherent TPIF was compared with the coherent homodyne-detected SFG. The second-order parametric model does not apply to a single molecule incoherent response and has to be extended to the fifth-order generalized response function description. Two photon fluorescence with one quantum and two classical modes (TPIF) is described not only by the causal response function $\chi^{(5)}_{+-----}$ but also by the second moment of molecular fluctuation $\chi^{(5)}_{++----}$. The two photon fluorescence signal with two quantum and one classical modes (TPEF) does not depend on the CRF but involves higher moments in material fluctuations $\chi^{(5)}_{+++---}$ and $\chi^{(5)}_{++++--}$.

For ensembles of identical molecules, such as crystals with no inversion symmetry, the SNGF corresponding to TPIF can be reduced to the homodyne-detected SFG given by the ordinary second-order response function $\chi^{(2)}_{+--}$. PDC is the coherent analogue of TPEF. In addition to the CRF $\chi^{(2)}_{+--}$, PDC contains contributions from the second moment of molecular fluctuations $\chi^{(2)}_{++-}$.

Equations (31) and (38) represent closed compact expressions for both coherent and incoherent signals involving one and two quantum modes, respectively. In the off-resonant regime, both types of PDC are well described by conventional second-order CRF. Quantum corrections quantitatively affect the Type II PDC but bring qualitative changes into Type I PDC in the vicinity of molecular resonances.

In this paper we have considered only one type of non-classical optical field—spontaneously emitted photons. Future applications to other types of non-classical fields such as, for instance, entangled photons, are of great interest [27]. The SNGF formalism shows that non-causal contributions to the nonlinear signals are signatures of various moments of molecular fluctuations.

Finally, we summarize the main advantages of the SNGF formalism.

- Processes involving an arbitrary number of classical and quantum modes of the radiation field may be treated within the same framework by simply varying the number of $+$ and $-$ superoperators.
- Intuitive loop diagrams can be used to describe all processes in the L, R representation.
- Incoherent and coherent (cooperative) signals may be derived from the same expressions.
- A unified approach is provided for resonant and off-resonant measurements. Only the latter may be described by an effective Hamiltonian for the field which depends parametrically on the matter.
- Nonlinear spectroscopy conducted with resonant classical fields only accesses the CRF. Quantum fields reveal the broader family of SNGFs which carry additional information about fluctuations, as shown in Table 1.
- Spectroscopy with quantum entangled fields [28,29] may be naturally described by the SNGF formalism.

Table 1. SNGFs for three-wave mixing techniques: heterodyne-detected SFG and DFG with all classical modes (c); incoherent TPIF with two classical and one quantum (q) mode and corresponding coherent homodyne-detected SFG; incoherent TPEF with one classical and two quantum modes and Type I PDC; Type II PDC SNGF with one classical and four quantum modes.

	Three wave processes					
	Heterodyne		Homodyne			
			Incoherent		Coherent	
Technique:	SFG	DFG	TPIF	TPEF	SFG	PDC
Modes:	c/c/c	c/c/c	c/c/q	c/q/q	c/c/q	c/q/q
ω_3:	$\omega_1+\omega_2$	$\omega_1-\omega_2$	–	–	$\approx \omega_1+\omega_2$	$\approx \omega_1-\omega_2$
Argument:	$(-\omega_3;\ \omega_2,\omega_1)$	$(-\omega_3;\ -\omega_2,\omega_1)$	$(-\omega_3;\ \omega_3,\omega_2,-\omega_2,\omega_1,-\omega_1)$	$(-\omega_3;\ \omega_3,-\omega_2,\omega_2,\omega_1,-\omega_1)$	$(-\omega_3;\ \omega_2,\omega_1)$	$(-\omega_3;\ -\omega_2,\omega_1)$
SNGFs	$\chi^{(2)}_{+--}$	$\chi^{(2)}_{+--}$	$\chi^{(5)}_{++----}-$	$-\chi^{(5)}_{++----}-\chi^{(5)}_{+++---}+$	$\lvert\chi^{(2)}_{+--}\rvert^2$	$\lvert\chi^{(2)}_{+--}+\chi^{(2)}_{++-}\rvert^2$
+, −			$-\chi^{(5)}_{+-----}$	$+\chi^{(5)}_{++-+--}+\chi^{(5)}_{++++--}$		
SNGFs mixed	–	–	$\chi^{(5)}_{\mathrm{LR}----}$	$\chi^{(5)}_{\mathrm{LRLR}--}$	–	–
SNGFs	$\chi^{(2)}_{\mathrm{LLL}}$	$\chi^{(2)}_{\mathrm{LLL}}-$	$\chi^{(5)}_{\mathrm{LRLRLR}}$	$-\chi^{(5)}_{\mathrm{LRLRLR}}$	$\lvert\chi^{(2)}_{\mathrm{LLL}}\rvert^2$	$\lvert\chi^{(2)}_{\mathrm{LLL}}\rvert^2$
L,R		$-\chi^{(2)}_{\mathrm{LRL}}$				
Expression	Equation (20)	Equation (18)	Equation (26)	Equation (34)	Equation (20)	Equation (36); Equations (39) and (41)

Acknowledgements

This work was supported by National Science Foundation grant CHE-0745892 and National Institutes of Health grant GM59230.

References

[1] C. Gerry and P. Knight, *Introductory Quantum Optics* (Cambridge University Press, Cambridge, 2005).
[2] M. Scully and M. Zubairy, *Quantum Optics* (Cambridge University Press, Cambridge, 1997).
[3] R. Glauber, *Quantum Theory of Optical Coherence: Selected Papers and Lectures* (Wiley–VCH, Weinheim, 2007).
[4] S. Mukamel, *Principles of Nonlinear Optical Spectroscopy* (Oxford University Press, New York, 1995).
[5] N. Bloembergen, *Nonlinear Optics* (World Scientific, Singapore, 1996).
[6] A.E. Cohen and S. Mukamel, Phys. Rev. Lett. **91** (23), 233202 (2003).
[7] U. Harbola, J. Maddox, and S. Mukamel, Phys. Rev. B **73** (20), 205404 (2006).
[8] C.A. Marx, U. Harbola, and S. Mukamel, Phys. Rev. A **77** (2), 022110 (2008).
[9] U. Harbola and S. Mukamel, Phys. Rep. **465** (5), 191 (2008).
[10] Y. Shen, Nature **337** (6207), 519 (1989).
[11] B. Dick and R. Hochstrasser, J. Chem. Phys. **78**, 3398 (1983).
[12] L. Mandel and E. Wolf, *Optical Coherence and Quantum Optics* (Cambridge University Press, Cambridge, 1995).
[13] C.K. Hong and L. Mandel, Phys. Rev. A **31** (4), 2409 (1985).
[14] D. Klyshko, *Photons and Nonlinear Optics* (Gordon and Breach, New York, 1988).
[15] W.H. Louisell, A. Yariv, and A.E. Siegman, Phys. Rev. **124** (6), 1646 (1961).
[16] K. Edamatsu, Jap. J. Appl. Phys. **46** (11), 7175 (2007).
[17] A. U'Ren, R. Erdmann, M. de la Cruz-Gutierrez, and I. Walmsley, Phys. Rev. Lett. **97** (22), 223602 (2006).
[18] W. Denk, J. Strickler, and W. Webb, Science **248** (4951), 73 (1990).
[19] C. Xu and W. Webb, J. Opt. Soc. Am. B **13** (3), 481 (1996).
[20] P.R. Callis, J. Chem. Phys. **99**, 27 (1993).
[21] A. Rehms and P. Callis, Chem. Phys. Lett. **208** (3/4), 276 (1993).
[22] U. Harbola, J. Maddox, and S. Mukamel, Phys. Rev. B **73** (7), 75211 (2006).
[23] D. Andrews and P. Allcock, *Optical Harmonics in Molecular Systems* (Wiley–VCH, Weinheim, 2002).
[24] T. Chui and K. Wong, J. Chem. Phys. **109**, 1391 (1998).
[25] C. Xu, J. Shear, and W. Webb, Anal. Chem. **69**, 1285 (1997).
[26] M.H. Rubin, D.N. Klyshko, Y.H. Shih, and A.V. Sergienko, Phys. Rev. A **50** (6), 5122 (1994).
[27] O. Roslyak and S. Mukamel, Opt. Express **17** (2), 1093 (2009).
[28] A. Pe'er, B. Dayan, A.A. Friesem, and Y. Silberberg, Phys. Rev. Lett. **94**, 073601 (2005).
[29] D. Lee and T. Goodson, J. Phys. Chem. B **110** (51), 25582 (2006).

Appendix A. Superoperator algebra

Below we briefly summarize superoperators and their algebraic properties [8].

The superoperators are defined by their action on an ordinary operator X:

$$A_- X = \frac{1}{\sqrt{2}}[A, X], \tag{A1}$$

$$A_+ X = \frac{1}{\sqrt{2}}(AX + XA). \tag{A2}$$

The following properties can be verified directly from the definition:

$$\langle AX\rangle = \langle A_+ X\rangle, \quad \langle A_- X\rangle = 0, \tag{A3}$$

$$(AB)_- = A_- B_+ + A_+ B_-, \quad (AB)_+ = A_+ B_+ + A_- B_-. \tag{A4}$$

The L(left),R(right) superoperators are given by their action in the Hilbert space:

$$A_{\mathrm{L}} X = AX, \quad A_{\mathrm{R}} X = XA.$$

The L,R and $+$, $-$ superoperators are related by the unitary transformation

$$A_- = \frac{1}{\sqrt{2}}(A_{\mathrm{L}} - A_{\mathrm{R}}), \quad A_+ = \frac{1}{\sqrt{2}}(A_{\mathrm{L}} + A_{\mathrm{R}}),$$
$$A_{\mathrm{L}} = \frac{1}{\sqrt{2}}(A_+ - A_-), \quad A_{\mathrm{R}} = \frac{1}{\sqrt{2}}(A_+ + A_-).$$

Appendix B. Rules for the CTPL diagrams

The following rules are used to construct the loop diagrams [8].

(1) Time runs along the loop clockwise from bottom left to bottom right.
(2) The left branch of the loop represents the ket, the right represents the bra.
(3) Each interaction with a field mode is represented by a line acting on either the right (R operators) or the left (L operators) branch.
(4) The field is marked by dressing the lines with arrows, where an arrow pointing to the right (left) represents the field annihilation (creation) operator $E_\alpha(t)$ ($E^\dagger_\alpha(t)$).
(5) Within the RWA, each interaction that annihilates a photon $E_\alpha(t)$ is accompanied by the operator $V^\dagger_\alpha$, which leads to molecular excitation. Similarly, $E^\dagger_\alpha(t)$ de-excites the molecule by applying operator V.

(6) Arrows pointing 'inwards' (i.e. pointing to the right on the ket and to the left on the bra) consequently cause absorption of a photon by exciting the system, whereas arrows pointing 'outwards' (i.e. pointing to the left on the bra and to the right on the ket) represent de-excitation of the system by photon emission.

(7) The observation time, t_{m+1}, is fixed and is always chronologically the last. As a convention, it is chosen to occur from the left. This can always be achieved by a reflection of all interactions through the center line between the ket and the bra, which corresponds to taking the complex conjugate of the original correlation function.

(8) The loop translates into an alternating product of interactions (arrows) and free evolution periods (vertical solid lines) along the loop.

(9) Since the loop time goes clockwise along the loop, periods of free evolution on the left branch amount to propagating forward in real time with the propagator given by the retarded Green's function G. Evolution on the right branch corresponds to backward propagation (advanced Green's function $G^{\dagger}$).

(10) The frequency arguments of the various propagators are cumulative, i.e. they are given by the sum of all 'earlier' interactions along the loop. Additionally, the ground-state frequency is added to all arguments of the propagators.

(11) The Fourier transform of the time-domain propagators adds an additional factor of $i(-i)$ for each retarded (advanced) propagator.

(12) The overall sign of the SNGF is given by $(-1)^{N_R}$, where N_R is the number of R superoperators.